Available online at www.sciencedirect.com
ScienceDirect
Journal of Non-Crystalline Solids 353 (2007) 658–662
JOURNAL OF NON-CRYSTALLINE SOLIDS
www.elsevier.com/locate/jnoncrysol

Observation of HfO_2 thin films by deep UV spectroscopic ellipsometry

F. Ferrieu [a,*], K. Dabertrand [a], S. Lhostis [a], V. Ivanova [b], E. Martinez [b], C. Licitra [b], G. Rolland [b]

[a] STMicroelectronics, 850 rue Jean Monnet, F-38926 Crolles cedex, France
[b] CEA-LETI, 17 rue des Martyrs, 38054 Grenoble, France

Available online 15 February 2007

Abstract

Deep UV spectroscopic ellipsometry (SE) is used for structure change observations in thin hafnia (HfO_2) layers deposited by p-MOCVD on silicon substrate. The absorption edge E_g and most of the critical point transitions in HfO_2 are above 6 eV, which makes the extension to Deep UV SE (5–9 eV) very suitable. The phase mixture changes as function of thickness and deposition process temperature, deduced from SE correspond well to XRD and Angle Resolved (AR)-XPS spectroscopy observations. From the absorption spectra at 4.5 eV, defects such as oxygen vacancies are detected, whereas from XPS spectra the estimation of the O/Hf ratio follows the same trend. Deep UV SE reveals differences in the dielectric function with orthorhombic/monoclinic phase mixtures essentially with peaks at 7.5 and 8.5 eV. Quantum confinement originated from the grain size of the films and the excitonic origin of the 6 eV feature are discussed.
© 2007 Elsevier B.V. All rights reserved.

PACS: 78.66.w; 07.60.−j; 71.30.+h

Keywords: UPS/XPS; X-ray diffraction; Dielectric properties, relaxation, electric modulus; Ellipsometry; Optical properties

1. Introduction

Ultra thin hafnia (HfO_2) films are used as high-k materials to improve device performance [1]. These layers must fulfill severe criteria, where the major issues concern the mobility and intrinsic or interfacial active defects. Their optical properties [2,3], dielectric constant and electrical properties are strongly dependant of the microstructure. The hafnia films are known to be stabilized in one specific phase following film stress, grain size effects and impurities. Hafnia and its twin oxide zirconia (ZrO_2) [4] have four phases (polymorphs): monoclinic, tetragonal, orthorhombic and cubic which can be stabilized by defects or Rare Earth (RE) doping elements. In the bulk only the monoclinic phase is stable at room temperature. The monoclinic to tetragonal phase transition occurs in bulk at 1720 °C. In thin films, the monoclinic phase transforms to the tetragonal or orthorhombic and eventually to the cubic (transitions at much lower temperatures 500–900 °C). Recently, Ushakov et al. [5] have used DSC calorimetry to measure the enthalpy of hafnia, as function of polymorphism. The crystallization pathways of zirconia or hafnia films are result of a thermodynamic martensitic stabilization [6]. It has been predicted that the tetragonal form can be stabilized at room temperature when the particles size is less than 30 nm [7] (a size greater than most of the film thicknesses discussed in this work).

Optical properties were observed in ALD films with large crystallites grain size [8,9]. However, beside the determination of the real optical band gap of hafnia no simple recognition of the micro-structural influence has been reported. Deep ultra violet spectroscopic ellipsometry (DUVSE) enables for structure change observation in thin hafnium oxide layers (as HfO_2 phases and associated defects).

* Corresponding author. Tel.: +33 4 38784056.
E-mail address: frederic.ferrieu@cea.fr (F. Ferrieu).

0022-3093/$ - see front matter © 2007 Elsevier B.V. All rights reserved.
doi:10.1016/j.jnoncrysol.2006.10.032

2. Experimental

2.1. Samples preparation

The Pulsed Metal Organic Chemical Vapor Deposition (p-MOCVD) technique is used for the growth of thin HfO_2 layers with hafnium-bis-butoxide-bis-(1-methoxy-2-methyl-2-propanolate) as precursor. A fine tuning injection provides low carbon content in the hafnia films. The films are grown at 550 °C and 430 °C on Si(100) wafers. The Si substrates were first HF-RCA processed which leads to a 0.7 nm-thick chemical oxide SiO_2 layers.

2.2. Characterization techniques

Measurements have been performed with two Spectroscopic Ellipsometers (SE) systems. The former is a 70° incidence angle Phase Modulated SE Ellipsometer from the low photon energy range (1.5 eV, i.e., 850 nm) up to 8 eV (150 nm). The second, a home-build rotating polarizer SE system, is a 55° up to 75° variable incidence angle SE with an enhanced and extended spectral resolution in the deep UV (120–600 nm) using a photon counting detection level.

Beside optical characterization, the samples morphology has been analyzed with Angle-Resolved X-ray Photoelectron Spectroscopy (AR-XPS) and X-ray Diffraction (XRD). AR-XPS measurements were performed in conditions allowing an optimal sensitivity respectively to the HfO_2 layers. XRD uses Cu anticathode X-ray source.

3. Results

3.1. Material properties

The structure and the crystalline polymorphs in thin films are not clearly pointed out until now in the literature [8,9]. ALD films, grown at 450 °C and 700 °C are found to be always in the monoclinic phase, whereas the films deposited by p-MOCVD at lower temperature contain also tetragonal crystallites. The presence or absence of an additional very specific absorption infrared band at 770 cm^{-1} in the Attenuated Total Reflection (ATR) measurements [10] is the unique evidence for the different phases in the structure of HfO_2 films grown by p-MOCVD. The structural properties of HfO_2 dielectrics are divided in three regions (Fig. 1). The first one, the lower area corresponds to amorphous films (A) or layers composed of nano-crystals. In the second region is presented a preferential mixture of the orthorhombic and monoclinic phases. The films (thicker than 6 nm) are deposited in the temperature range 400–500 °C. In the third region (the upper right area) the HfO_2 layers (deposited at temperatures higher than 500 °C) are only in the monoclinic phase (M). However, the delimitation between second region and third remains unclear (dot line). We have studied the optical properties of the associated phase mixtures as a function of thickness and temperature. The samples have been chosen from these three regions. In the first set, the films are deposited at 430 °C, with thicknesses of 3.5 nm, 9.5 nm and 12.7 nm. The second set consists of 3 and 5 nm thick HfO_2 films, grown at 550 °C. The samples are identified in the following way: the temperature and the thickness are appended together with the phase nature abbreviation respectively to amorphous (A), orthorhombic (O), monoclinic (M) and mixed phase (OM).[1]

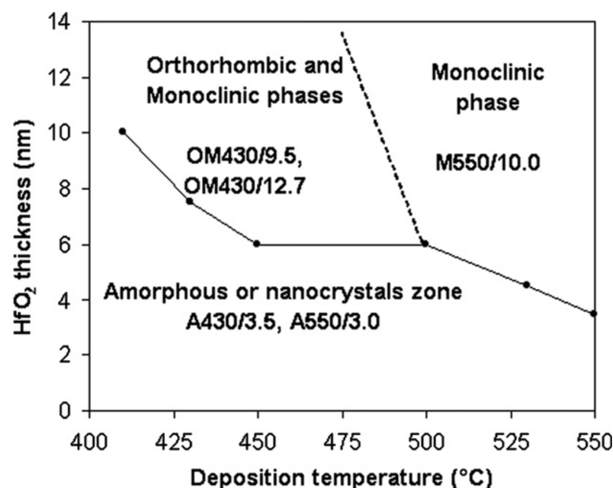

Fig. 1. Identification of the HfO_2 phase mixtures, in layers grown by p-MOCVD, as a function of the deposition temperature and thickness according to infrared Attenuated Total Reflection (ATR) and XRD.

3.2. X-ray investigation and AR-XPS

The XRD diagram of HfO_2 9.5-nm thick sample grown at 430 °C (OM430/9.5) reveals a phase mixing: one diffraction peak related to the monoclinic phase and three others diffraction peaks which point out the orthorhombic phase, all increasing with thickness. Finally, in thicker films grown at 430 °C, the two phases are present but with a higher proportion of monoclinic. The HfO_2 films grown at higher temperature ($\geqslant$500 °C) are only in the monoclinic phase (M550/10). The AR-XPS method emphasizes the bonding states character into HfO_2 layers:

(1) For all samples: OM430/9.5, OM550/10.0, OM430/12.7, A430/3.5, and A550/3.0, in the Hf 4f core level spectra, is observed a unique $4f_{7/2}$–$4f_{5/2}$ component with a binding energy of around 17–18 eV related to Hf–O bonds. For the thicker films, the Hf 4f core level spectra slightly shifts towards the highest binding energy, from 17.73 eV up to 17.91 eV, a probable indication for change in the binding environment due to phase modification. A similar effect is observed for the samples deposited at 550 °C (A550/3 and OM550/10).

[1] For example: A430/3.5 is an amorphous sample of 3.5-nm thick deposited at 430 °C.

Table 1
Ratio of oxygen/Hf estimated from XPS O 1s and the Hf 4f core level spectra versus film thickness, deposition temperature, grain size and film density

Deposition temperature (°C)	Samples	Thickness (nm)	O/Hf ratio (XPS)	Grains size (nm)	Density (g/cm^3)
430	A430/3.5	3.5	1.3	Amorphous	8.6
430	OM430/9.5	9.5	1.9	7 ± 0.5	9.3
430	OM430/12.7	12.7	1.9	10 ± 1	–
550	A550/3	3	1.6	Amorphous	9.4
550	OM550/10	10	1.7	8 ± 0.5	9.7

(2) From the O 1s core level spectra, and the Hf 4f core level spectra, the ratio O/Hf is estimated. However with thickness less than 1 nm, the interfacial native oxide layer affect considerably this integration procedure and an unrealistic lower oxygen contents are observed (see Table 1).

3.3. Spectroscopic ellipsometry approach

The measurements below the strong absorption onset are used to determine the film thickness. The classical Tauc Lorentz (TL) formalism limited to the 1.5–8 eV spectral range, is applied to ensure a Kramers–Krönig (KK) consistent model. In order to avoid some possible correlations between the parameters, the optical dielectric function ε_1 and ε_2, (respectively real and imaginary part of ε), are then recalculated and compared together (Fig. 2 continuous curves). For each sample, the imaginary part of the dielectric function $\varepsilon_2(\omega)$ is reported versus the photon energy ω (eV). When considering the thin and thick samples, large differences between the respective dielectric function emerge. For instance, their shapes reveal an initial amorphous wide absorption band and structure-less state (A430/3.0 and A550/3.0). In $\varepsilon(\omega)$ an additional component, (i.e. here 2TL are needed), has to be supplied for the orthorhombic/monoclinic mixed phases (OM430/95 and OM430/12.7). Moreover, the film densifies with the increasing nucleation of the crystallites, leading to higher values of the dispersive component.

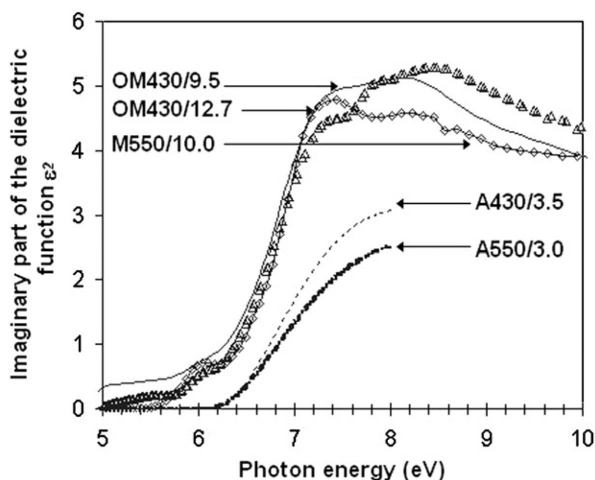

Fig. 2. Imaginary part of the dielectric function $\varepsilon_2(\omega)$ calculated from the Tauc–Lorentz models (A550/3.0, A430/3.5) and by n, k inversion (M550/10.0, OM430/12.7 and OM430/9.5) versus energy (eV).

The shoulder observed around 6 eV reveals a transition arising with the poly-crystalline nucleation and growth whatever the film phase nature is (seen for OM430/9, OM430/12.7, M550/10). Such a singularity has been previously observed in ALD films with an increasing sharpness when annealing [9–11]. It has been identified, as the E_g, T_{2g} states in the band diagram of crystal field splitting hypothesis [12]. In the high-energy range (VUV range) up to ~10 eV, the optical indices n, k (and $\varepsilon(\omega)$ as well), can be directly extracted by numerical inversion from the Δ, Ψ ellipsometry angles measured with the second VUV-SE. The imaginary part of $\varepsilon(\omega)$ has similar characteristics as earlier published results [8,9,11]. Hardly resolved with the first SE measurements in the 8.0 eV range, here the two maxima corresponding to the transition features T_{2g} and E_{2g} are clearly outlined (M550/10) [12]. The HfO_2 structure has two optical transitions at 7.5 and 8.2 eV, assigned to the monoclinic phase of HfO_2 (M550/10). With a high concentration of orthorhombic crystallite (OM430/10), only one optical transition (8.2 eV) is observed, while monoclinic crystallites are in a very beginning nucleation phase, (OM430/12.7). A relative loss of the optical structure indicates a partial transformation back to the monoclinic rearrangement with an increase of the film thickness.

4. Discussion

4.1. Quantum size effect

Quantum size effects [13] are invoked in the case of the absorption band tail and several arguments favoured it. Furthermore: (i) in thin samples, are necessary more than two 2TL to see a slow decrease of the absorption coefficient. Similarly to the absorption coefficient $\alpha(\omega)$ [12], shifts of the edge of the absorption tail are observed for $\varepsilon_2(\omega)$ (Fig. 2). According to the XRD analysis, p-MOCVD deposition method yields a much lower grain size value (less than 10 nm) than previous techniques. With such a size, the quantum confinement effects are expected to modify the absorption spectrum leading to a blue shift of the absorption edge while grain size decreases. This shift is the clearest known evidence for a quantum confinement effect given in the literature [13,14].

(ii) The absorption edges versus grain sizes values are compared (Fig. 3) with the expression derived for the band gap energy when quantum confinement is present and adjusted in the case of RE doped zirconia [13]. It has been found that:

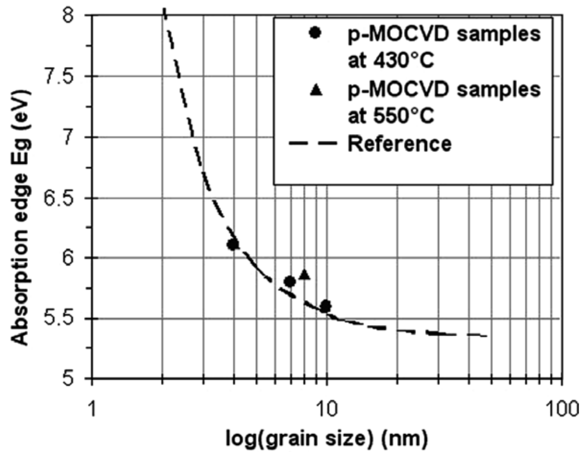

Fig. 3. The absorption edge E_g (eV) versus logarithm of grain size (nm) compared with the numerical curve deduced from quantum confinement theory.

$$E_g\ (\text{eV}) = 5.62 + 8.68/d_g^2 + 1.24/d_g$$

where d_g (nm) is the crystallite size, represented by the continuous curve (Fig. 3). Indeed, the two materials remain with identical crystal phases and similar grain size which permits to use this analytical expression in term of comparison. The general trend, predicted by the quantum model, correlates perfectly with the experimental data. Finally it can also explain the unsuccessful attempt to fix the onset of absorption with a Tauc or Cody-Lorentz plot [3]. Many authors doubt on the nature of the 6 eV absorption features where several hypotheses are proposed: crystal field splitting, quantum size effect or excitonic absorption. The last possible assumption is emphasized from the photoluminescence (PL) data. Self trapped excitons induce emission bands at 3.3 and 4.4 eV, are visible as well as at 10 K and at room temperature [9]. The shape and sharpness of the pseudo band-edge at 6 eV are influenced from the differences in the film morphology and thickness. In the SE data, the addition of Wannier exciton dispersion at 6 eV to the Tauc–Lorentz oscillator model leads to a perfect agreement with the ellipsometry data [15].

4.2. Crystal impurities and presence of oxygen vacancies

Some other absorptions features are observed at low photons energies. The features observed at 5.5 eV (Fig. 4), have also been reported by Takeuchi [8]. For ALD films, these features disappear with a high temperature under oxygen annealing [11]. In order to insure more precise information, the measurements were performed with different SE. The absorption peaks detected at lower energy range (3.8–4.2 eV) have not been yet reported but they correspond to the bands also seen by PL. Unfortunately there are not other evidences for the real nature of these transitions. The effect is also related with film thickness and growth temperature. Disorder and defects affect consequently the optical properties of p-MOCVD hafnia films. Thus, for a given thickness, the HfO_2 films deposited at 550 °C, have more vacancies than the one deposited at 430 °C (Fig. 4). The AR-XPS films composition evaluation is well correlated to the decrease in the peak height at 4 eV of $\varepsilon_2(\omega)$ as observed by SE.

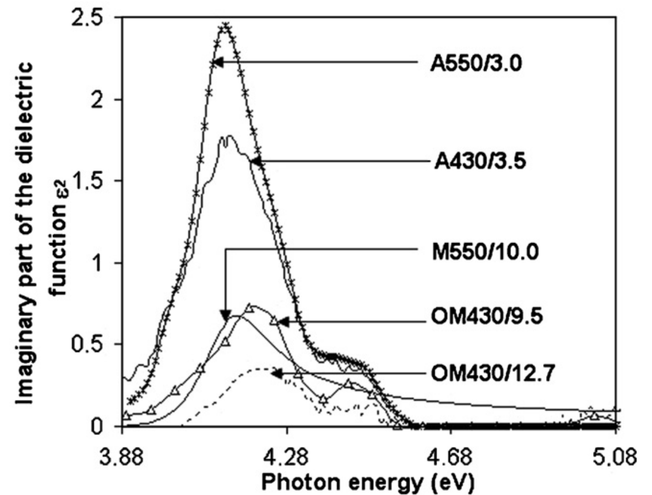

Fig. 4. The imaginary part of the dielectric function ε_2 versus photons energy (eV) where additional features at 3.8–5.5 eV range are seen by SE and confirmed also by PL measurements [7].

5. Conclusions

SE provides important information about structure changes in thin p-MOCVD hafnia films. The obtained results are consistent with each of the other techniques used in this study (XRD, XPS and ATR). With decrease in the film thickness an analytical TL is then no more sufficient as observed in the DUV range. Due to the crystallite size, a shift of the absorption edge occurs toward the high photon energy (>6 eV), fully compatible with a quantum size effect. The dielectric function corresponding to the mixture between orthorhombic and monoclinic phase, represents the natural crystalline morphology of the film. Some extra-absorptions inside the band edge are detected, presumed also from the PL measurements. The potential defects are mostly related to the oxygen vacancies than to the impurities in the films. Despite the various hypotheses a clear explanation about the nature of the band edge cannot be proposed.

References

[1] G.D. Wilk, R.M. Wallace, J.M. Anthony, J. Appl. Phys. 89 (2001) 5243.
[2] N.V. Edwards, in: Proceeding of Characterization and Metrology for ULSI Technology, 2003, p. 723.
[3] J. Price, P.Y. Hung, T. Rhoad, B. Foran, A. Diebold, Appl. Phys. Lett. 85 (2004) 1701.
[4] X. Zhao, D. Vanderbilt, Phys. Rev. B 65 (2002) 233106.
[5] S.V. Ushakov, A. Navrotsky, Y. Yang, S. Stemmer, K. Kukli, M. Ritala, M. Leskelä, P. Fejes, A. Demkov, C. Wang, B.-Y. Nguyen, D. Triyoso, P. Tobin, Phys. Stat. Sol. (b) 241 (2004) 2268.

[6] J. Tang, Adv. Funct. Mater. 15 (2005) 1595.
[7] R.C. Garvie, J. Phys. Chem. 82 (1978) 18.
[8] H. Takeuchi, H. Daewon, Tsu-Jae King, J. Vac. Sci. Technol. A 22 (2004) 1337.
[9] J. Aarik, H. Mändar, M. Kirm, L. Pung, Thin Solid Films 466 (2004) 41.
[10] N.V. Nguyen, A.V. Davydov, D. Chandler Horowitz, M. Frank, Appl. Phys. Lett. 87 (2005) 192903.
[11] Y. Cho, N. Nguyen, C. Richter, J. Ehrstein, B. Lee, J. Lee, Appl. Phys. Lett. 80 (2002) 7.
[12] G. Lucovsky, J. Lüning, in: Proceeding of ESSDERC Grenoble, France, 2005, p. 439.
[13] I. Kosacki, V. Petrovsky, H.U. Anderson, Appl. Phys. Lett. 74 (1999) 341.
[14] M. Losurdo, Thin Solid Films 455&456 (2004) 301.
[15] D.D. Sell, P. Lawaetz, Phys. Rev. Lett. 26 (1971) 311.